Supporting Information

Efficient preadsorption-degradation of PFOA in water by NaClO-assisted electrocoagulation technique using Fe/Ni foam electrode

Dan Zhang [a,b], Yiming Li * [a,b], Xiuping Chen [a,b], Jinlei Song [a,b], Hu Kang [a,b], Mutai Bao [a,b] and Zhining Wang * [c]

[a] Key Laboratory of Marine Chemistry Theory and Technology, Ministry of Education, Ocean University of China, Qingdao, 266100, P.R. China

[b] Colledge of Chemistry and Chemical Engineering, Ocean University of China, Qingdao, 266100, P.R. China

[c] Shandong Key Laboratory of Water Pollution Control and Resource Reuse, School of Environmental Science and Engineering, Shandong University, Jinan, 250100, P.R. China

* Corresponding authors.
  E-mail address: liym@ouc.edu.cn (Y.M. Li); wangzhn@sdu.edu.cn (Z.N. Wang).

Text S1: Materials

Ethanol (CH$_3$CH$_2$OH, ≥99.7%), nitrobenzene (NB, ≥99.5%), tertiary butanol (TBA, ≥98.0%), 2, 4, 5−trimethoxybenzoic acid (TMBA, ≥99.5%), benzoic acid (BA, ≥99.5%), sodium hydrate (NaOH, ≥96.0%), hydrochloric acid (HCl, 36%-38%) were purchased from Sinopharm Chemical Reagent Co., Ltd. (Shanghai, China). Perfluorooctanoic acid (PFOA, ≥96.0%) was purchased from Aladdin (China). Fe/Ni foams (size: 3 × 2 × 0.1 cm. The molar ratio of Fe/Ni is 7:3.) were purchased from Kunshan Electronic Materials Co., Ltd (Kunshan, China). All the reagent materials were analytical grade and used without further purification. Deionized water was used in the whole experiment.

Text S2: Analytical methods

The surface morphologies of Fe flocs were characterized by scanning electron microscopy (SEM, Hitachi S8200, Japan) and a high-resolution transmission electron microscope (HRTEM, FEI Tecni G30, USA). The chemical compositions and valence of elemental of the samples were characterized by the X-ray photoelectron spectra (XPS, K-alpha 250Xi, USA). Powder X-ray diffraction (XRD, D/max-2500PC, Japan) was performed to identify the crystal phase by using Cu-Kα radiation (λ = 0.154 nm). A Fourier-transform infrared spectrometer (FT-IR; Nicolet 6700; Thermo Scientific, USA) was used to determine the chemical characteristics of the floc samples. The metallic elemental composition in solution was measured by Inductively Coupled Plasma-Atomic Emission Spectrometry (ICP-AES, Agilent 730, USA). The pH was measured with a pH meter (310P-02, Thermo Fisher, USA). The zeta potentials of the Fe flocs in suspensions were measured using Zetasizer Nano ZS90 (Malvern Instruments, UK). To evaluate the mineralization of PFOA during the

electrocoagulation reaction, total organic carbon (TOC) was measured using a TOC-V_{CPH} analyzer (Shimadzu, Kyoto, Japan). The F^- concentration was determined by an ion meter (XSJ-216, Shanghai, China). The concentration of PFOA and its decomposition products were analyzed by High-Performance Liquid Chromatography (HPLC-MS) (Agilent 1290-UPLC 6550, USA) experiments, where water cortecs C_{18} column (2.1 × 50 mm, 1.7 μm) was used. The column oven temperature was set to 35 °C. The flow rate was maintained at 0.2 mL/min with a mobile phase of eluent A (2 mmol/L ammonium acetate/water) and B (methanol). The eluent gradient started with 20% A and 80% B for 2 min and then was linearly increased to 80% A and 20% B over 6 min. Chromatographically separated samples were analyzed in negative ion monitoring mode for PFOA (m/z = 412.97), PFHpA (m/z = 362.97), PFHxA (m/z = 312.97), PFPeA (m/z = 262.98), PFBA (m/z = 212.98), and PFPrA (m/z = 162.98). Operational conditions were as follows: the sheath gas (N_2) pressure was 0.4 MPa (35 psi), the capillary potential was −4.0 kV, the source temperature was 120 °C, and the desolvation temperature was 350 °C. An electrospray negative ionization mode was used to identify the products in the liquid phase. The analysis was carried out in multiple reaction monitoring modes.

Text S3: Scavenging tests

According to known literature reports, the degradation mechanism of PFOA during the EC-NaClO are divided into two parts, which are direct oxidation (direct electrolysis) and indirect oxidation (free radical reactions) [1]. There are •OH and various chlorinated active species (CAS) such as Cl•, Cl_2^-•, ClO• playing important roles in organics degradation. Therefore, the overall rate constant during the EC-NaClO can be expressed according to the following **Eq. (1)**:

$$k'_{PFOA} = k'_{EC\text{-}PFOA} + k'_{\bullet OH\text{-}PFOA} + k'_{CAS\text{-}PFOA} \tag{1}$$

where k'_{PFOA} is defined as the overall degradation rate constant of PFOA which can be obtained experimentally, $k'_{EC\text{-}PFOA}$, $k'_{\bullet OH\text{-}PFOA}$ and $k'_{CAS\text{-}PFOA}$ represent the pseudo-first-order degradation rate constants of PFOA degradation initiated by direct electrolysis, •OH and CAS radicals, respectively. $k'_{EC\text{-}PFOA}$ can be obtained in scavenging tests where TBA (0.5 M) can be quenched •OH and CAS radicals in the EC-NaClO system. The NB can only react with •OH with a rate constant of 3.9×10^9 M^{-1} s^{-1} and it has been used as the probe compound to obtain $k'_{\bullet OH\text{-}PFOA}$. $k'_{CAS\text{-}PFOA}$ can be calculated by the difference of others. The relative contribution of the direct electrolysis and free radical reactions for PFOA degradation can be expressed as $k'_{EC\text{-}PFOA}/k'_{PFOA}$ and $\left(k'_{\bullet OH\text{-}PFOA} + k'_{CAS\text{-}PFOA}\right)/k'_{PFOA}$ ($k'_{\bullet OH\text{-}PFOA}/k'_{PFOA}$ and $k'_{CAS\text{-}PFOA}/k'_{PFOA}$).

The second radicals (Cl$_2^-$• and ClO•) were created from the conversion reaction of the primary radicals (•OH and Cl•). But in the low concentration of chloride, Cl$_2^-$• is negligible. CAS mainly includes ClO• and Cl• radicals. The relative contributions of •OH, ClO• and Cl• were determined based on the steady-state assumption of radical concentration, the specific calculations are shown in the following **Eqs. (2-6)**.

$$k'_{PFOA} \tag{2}$$
$$= k'_{EC\text{-}PFOA} + k_{\bullet OH\text{-}PFOA}[\bullet OH]ss + k$$

$$-ln\frac{PFOA_t}{PFOA_0} = -ln\frac{NB_t}{NB_0} \times \frac{k_{\bullet OH\text{-}PFOA}}{k'_{\bullet OH\text{-}NB}} \tag{3}$$

$$-ln\frac{PFOA_t}{PFOA_0} = -ln\frac{TMBA_t}{TMBA_0} \times \frac{k_{ClO\bullet - PFOA}}{k'_{ClO\bullet - TMBA}} \tag{4}$$

$$[\bullet OH]ss = \frac{k'_{NB}}{k'_{\bullet OH - NB}} \tag{5}$$

$$[ClO\bullet]ss = \frac{k'_{TMBA}}{k'_{ClO\bullet - TMBA}} \tag{6}$$

where $k_{\bullet OH - PFOA}$, $k_{ClO\bullet - PFOA}$ and $k_{Cl\bullet - PFOA}$ represent the second order rate constant of $\bullet OH$, $ClO\bullet$ and $Cl\bullet$ reacting with PFOA. The second order rate constant of $\bullet OH$ and $ClO\bullet$ reacting with PFOA were calculated by **Eqs. (3-4)**. $[\bullet OH]ss$ and $[ClO\bullet]ss$ are defined as the steady-state concentration of $\bullet OH$ and $ClO\bullet$, which were calculated according to **Eqs. (5-6)**. k'_{NB} and k'_{TMBA} are overall degradation rate constant of NB and TMBA during the EC-NaClO and can be obtained experimentally. TMBA (0.25 mM) was selected as an in situ $ClO\bullet$ probe and the second-order rate constant for TMBA with $ClO\bullet$ is 1.1×10^9 M^{-1} s^{-1}.

To further investigate the reactivity between $Cl\bullet$ and PFOA, competing kinetic experiments were conducted using a mixed system of PFOA, NB and BA. NB could react with $\bullet OH$ rapidly, while its reactions with CAS were negligible. BA could react with both $\bullet OH$ and $Cl\bullet$ with rate constants of 5.9×10^9 and 1.8×10^{10} M^{-1} s^{-1}, respectively. The calculation method of the second-order rate constant of $Cl\bullet$ reaction with PFOA ($k_{Cl\bullet - PFOA}$) and $[Cl\bullet]ss$ was referenced by Wang et al[2]. The degradation kinetics of PFOA, NB, and BA can be given by experiments (k'_{PFOA}, k'_{NB} and k'_{BA}), the $k_{Cl\bullet - PFOA}$ can be expressed as equations as follows **Eqs. (7-9)**:

$$[\bullet OH]ss = \frac{k'_{NB}}{k'_{\bullet OH - NB}} \tag{7}$$

$$[\bullet Cl]ss = \frac{k'_{BA} - k'_{\bullet OH - NB} \times [\bullet OH]ss}{k'_{\bullet Cl - BA}} \tag{8}$$

$$k_{Cl\bullet - PFOA} = \frac{k'_{PFOA} - k'_{\bullet OH - PFOA} \times [\bullet OH]}{[\bullet Cl]ss} \tag{9}$$

Text S4: Data analysis

The electrical energy consumption (*EEC*) was calculated in terms of Wh/L of treated effluent using the equation given below **Eq. (10)** [3]:

$$EEC = \frac{USj}{V} \times t_{EC} \tag{10}$$

where U is the average cell voltage (V), S is the anode surface area (cm^2), j is the applied current density (mA/cm^2), t_{EC} is the EC treatment time (h), and V is the volume (mL) of effluents.

The current efficiency (η) of the EC process was expressed using the following **Eq. (11)**:

$$\eta = \frac{\Delta M_{exp}}{\Delta M_{theo}} \times 100\% \tag{11}$$

where ΔM_{exp} is the experimentally measured amount of metal dissolution during the the EC process (mg), and ΔM_{theo} is the theoretical amount of metal dissolution with Faraday's law with 100% current efficiency (mg). ΔM_{exp} and ΔM_{theo} can be calculated by the following **Eqs. (12-13)**:

$$\Delta M_{exp} = M_{before} - M_{after} \tag{12}$$

$$\Delta M_{theo} \ = \ 1000 \ \times \ \frac{3600 \times I \times M}{n \times F} \ \times \ t_{EC} \qquad \qquad \textbf{(13)}$$

where M_{before} is the weight of metal anode before EC (mg), and M_{after} is the weight of metal anode after EC (mg). I is the electrical current (A), M is the molecular weight of metal (g/mol), F is Faraday's constant (96485 C/mol), and n is the number of electrons moles.
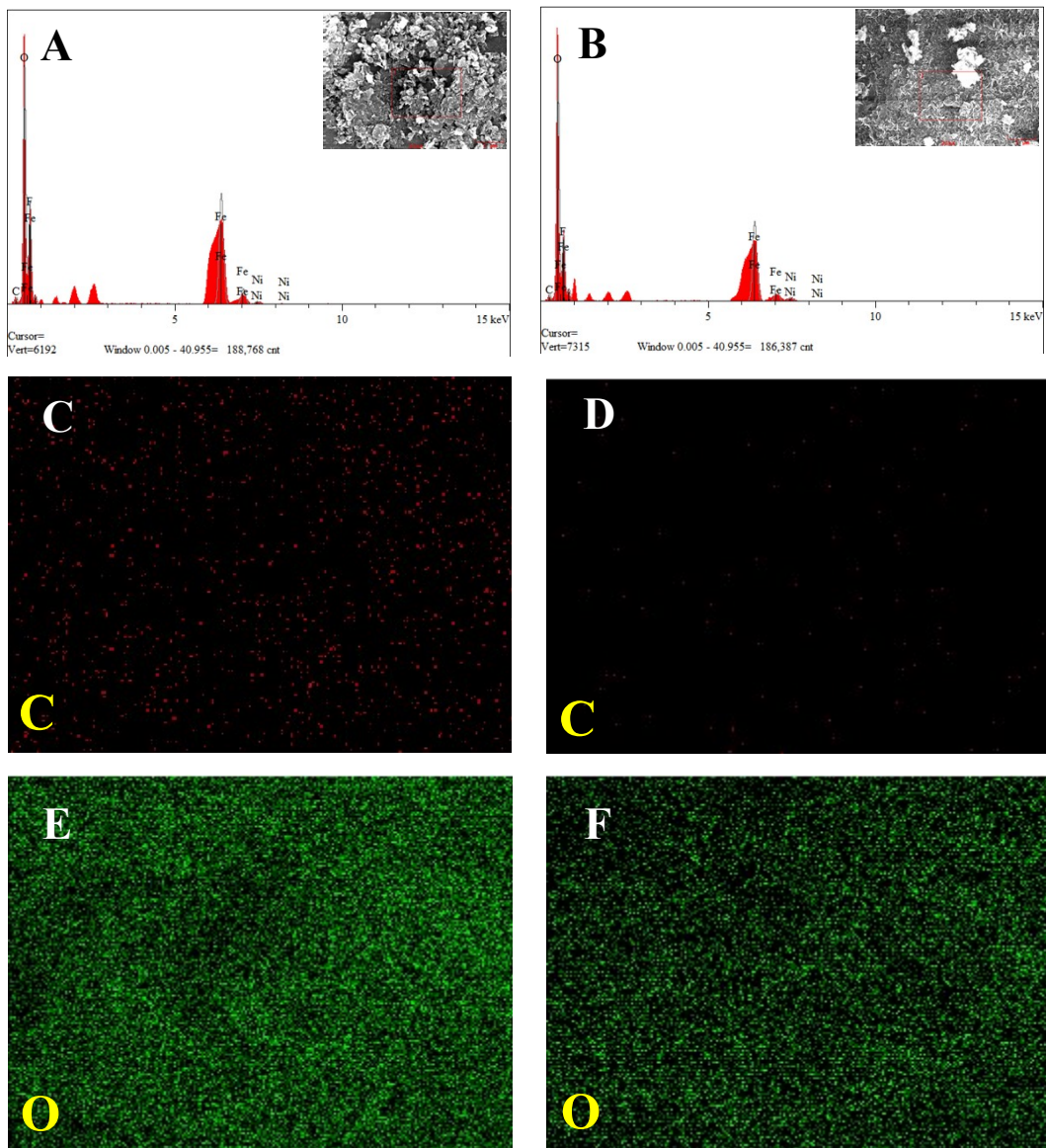
Figure S1. SEM-EDS elemental mapping images of flocs generated *in situ* using Fe/Ni foam electrode in the EC (A) EDS spectra; (C) C; (E) O and EC-NaClO process(B) EDS spectra; (D) C; (F) O.
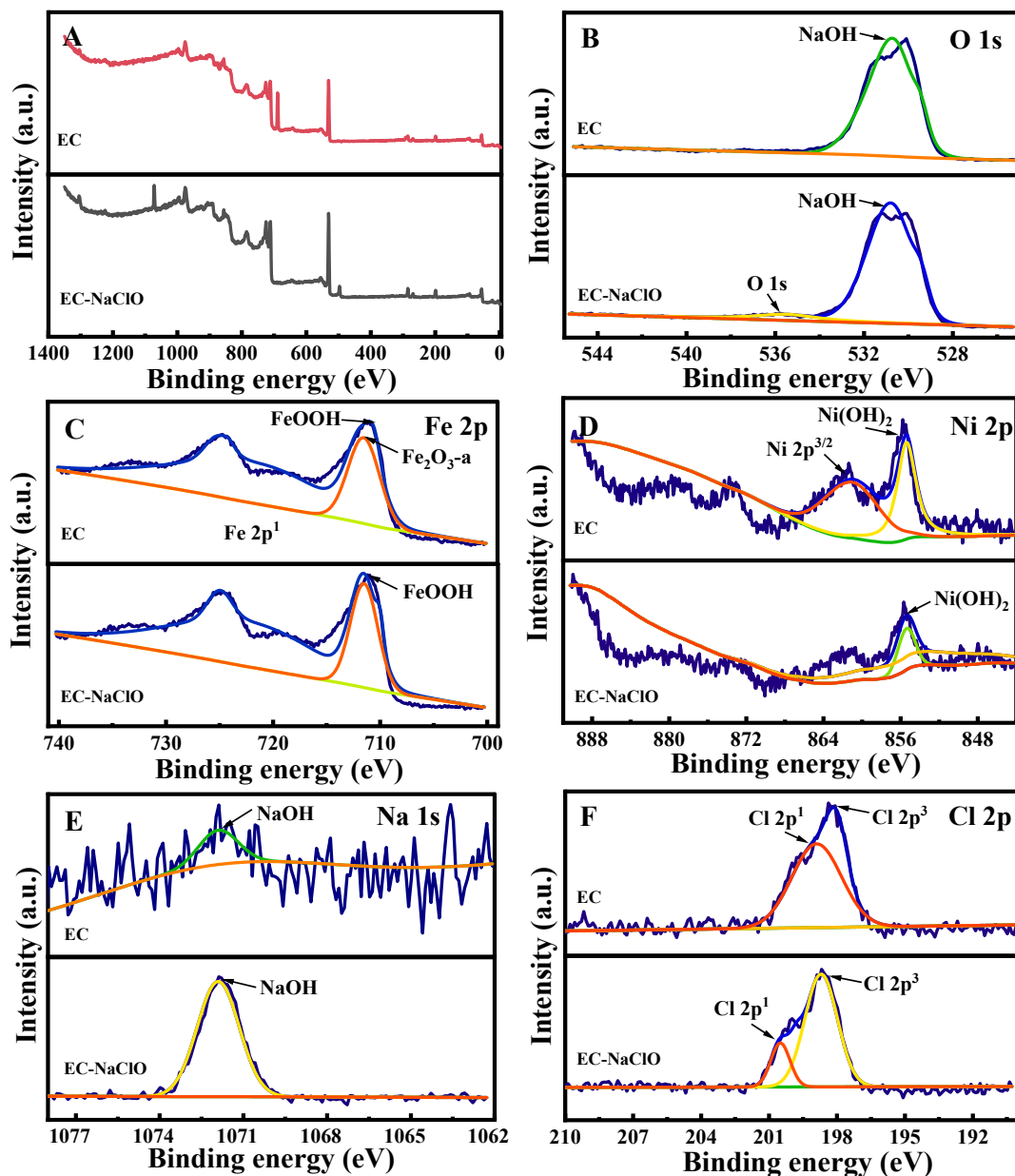
Figure S2. (A) XPS survey spectra; high resolution XPS spectrum of flocs generated *in situ* in the EC and EC-NaClO process using Fe/Ni foam electrode (B) Fe 2p, (C) Ni 2p, (D) Na 1s, (E) Cl 2p, (F) O 1s.
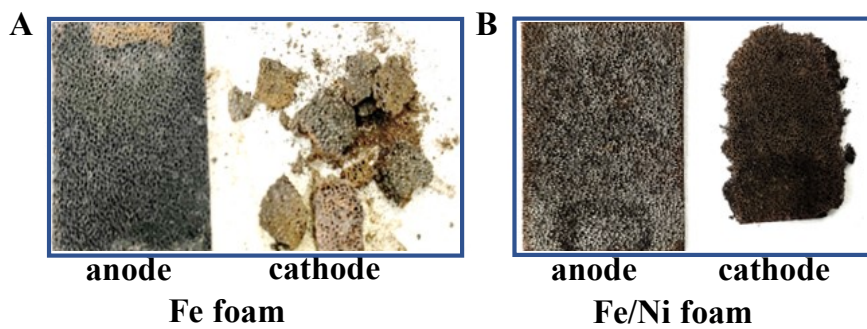
Figure S3. Photographs of the used electrode for the EC-NaClO degradation of PFOA after the three cycle experiments with (A) Fe foam and (B)Fe/Ni foam electrode.
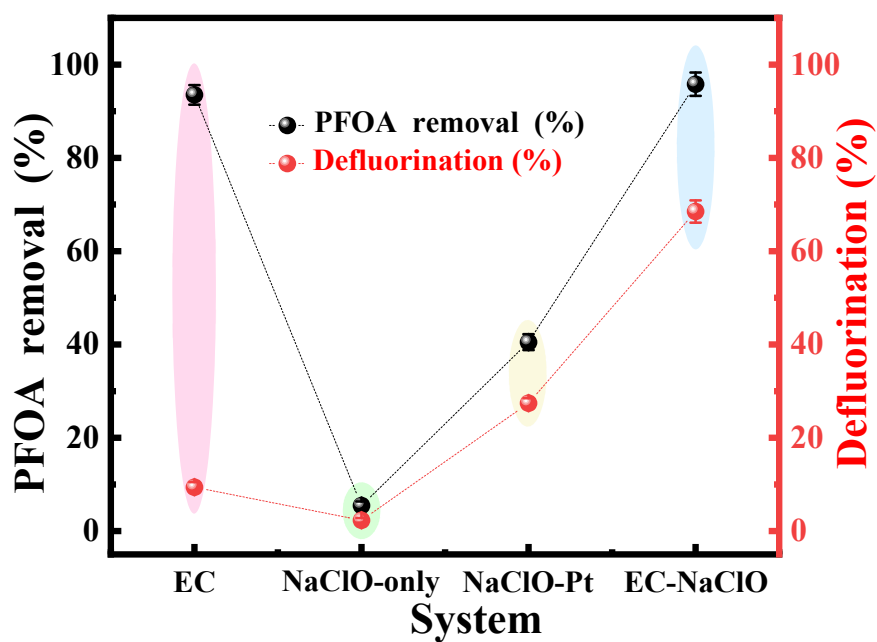
Figure S4. The removal and defluorination of PFOA in different systems. In these experiments, 100 mg/L PFOA was used. NaClO-only: NaClO was added but without current density. NaClO-Pt: NaClO and current density were applied.
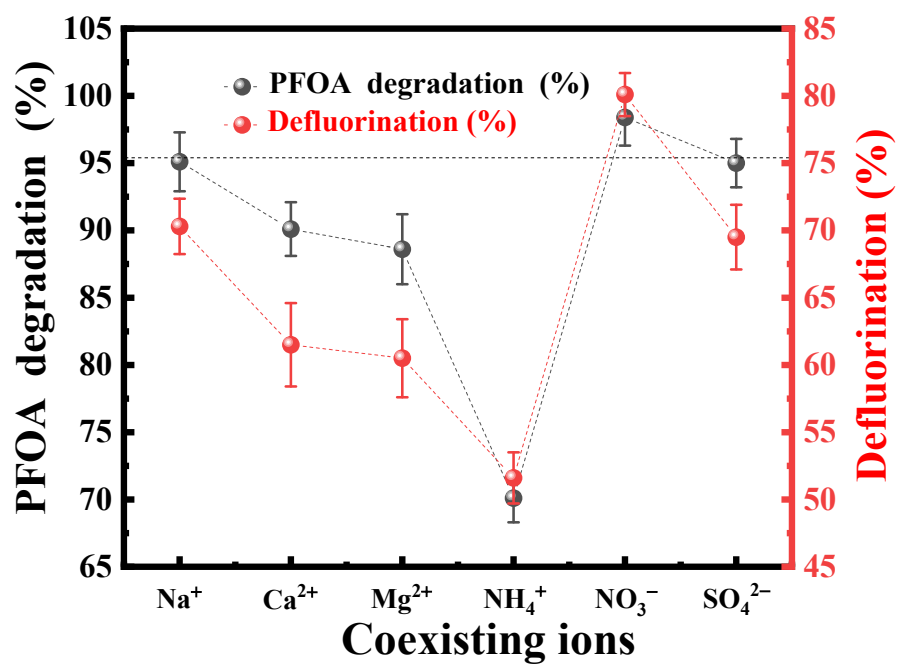
Figure S5. The degradation and defluorination of PFOA in the presence of 0.035 mol/L coexisting ion in the EC-NaClO system.
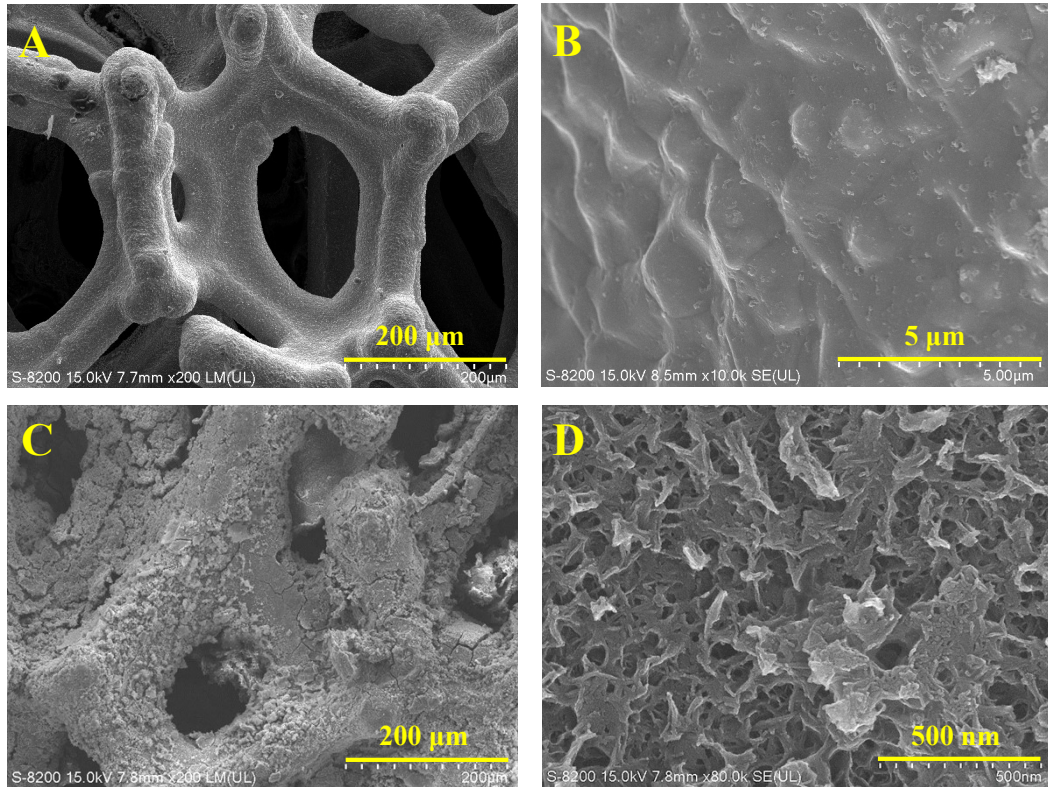
Figure S6. SEM patterns of the fresh (A, B) and used (C, D) foam Fe/Ni electrode for the EC-NaClO degradation of PFOA.
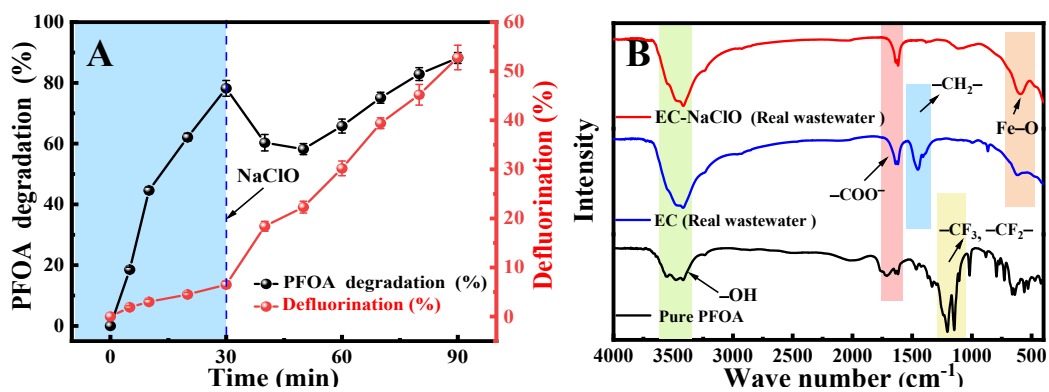
Figure S7. (A) The degradation and defluorination rate of PFOA after the EC-NaClO process in real factory wastewater; (B) FT-IR spectra of PFOA, Fe flocs generated *in situ* in the EC and the EC-NaClO process in real factory wastewater.

Equation	y = a + b*x
Plot	B
Weight	No Weighting
Intercept	5.47945E-5 ± 0
Slope	0.01253 ± 4.59
Residual Sum of S	0.00515
Pearson's r	0.99732
R-Square (COD)	0.99464
Adj. R-Square	0.9933
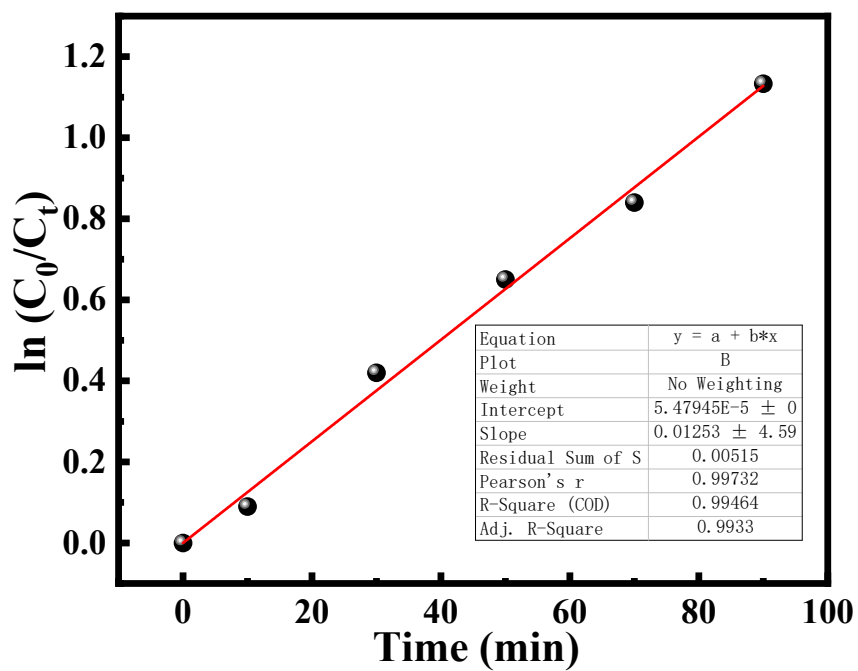
Figure S8. The degradation kinetics of NB in the EC-NaClO process.
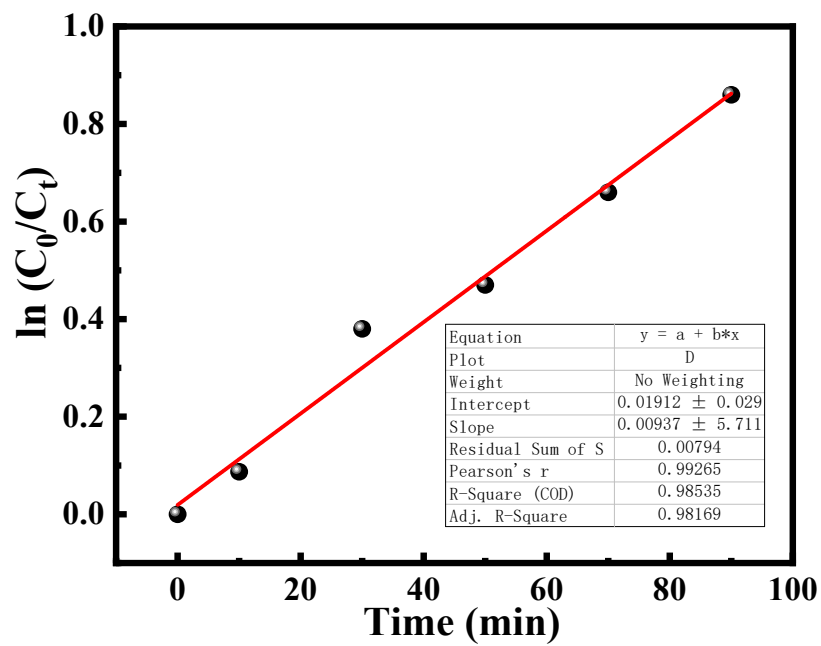
Figure S9. The degradation kinetics of TMBA in the EC-NaClO process.

Equation	y = a + b*x
Plot	D
Weight	No Weighting
Intercept	0.01912 ± 0.029
Slope	0.00937 ± 5.711
Residual Sum of S	0.00794
Pearson's r	0.99265
R-Square (COD)	0.98535
Adj. R-Square	0.98169
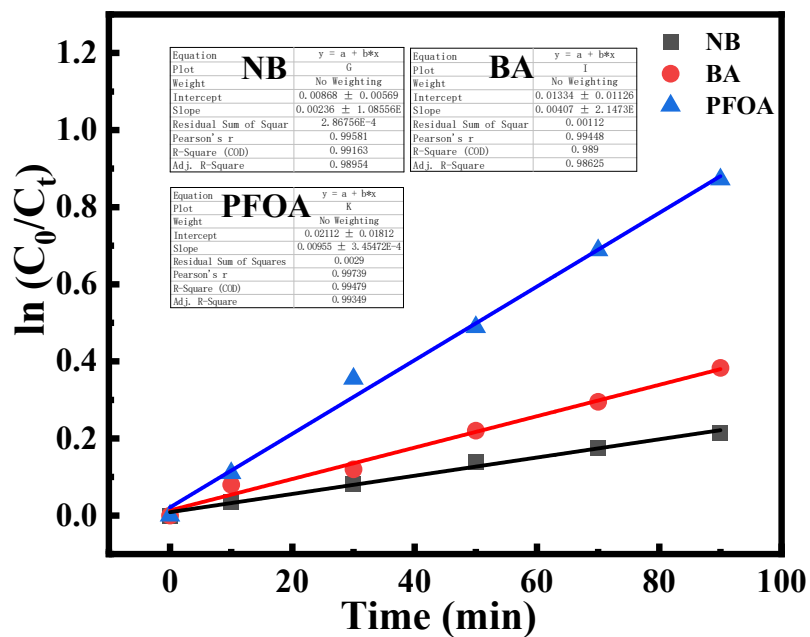
Figure S10. The degradation kinetics of TMBA in the EC-NaClO process. The degradation kinetics of PFOA, NB, and BA degradation versus in the mixed system of PFOA, NB and BA.
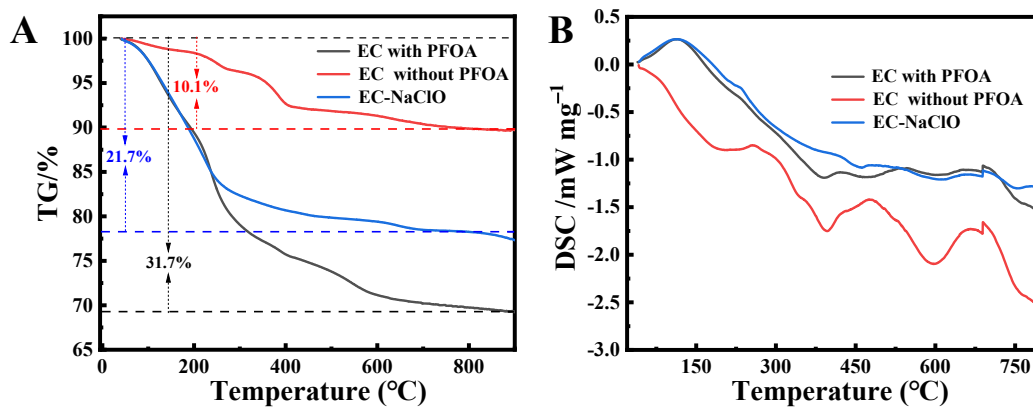
Figure S11. TG-DSC curves of flocs generated *in situ* in the EC and EC-NaClO with PFOA processes using Fe/Ni foam electrode.
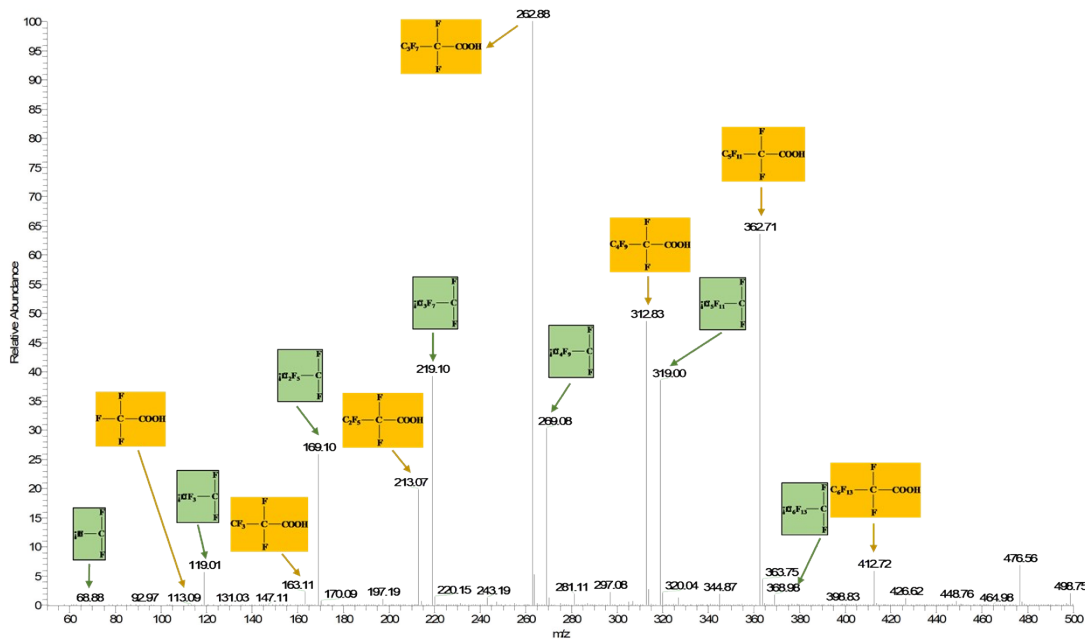
Figure S12. High resolution mass spectrometry spectra of PFOA degradation in the EC-NaClO process by Fe/Ni foam electrode.

Table S1. XRF analysis of Fe flocs generated in-situ in the EC and the EC-NaClO process using Fe/Ni foam electrode.

Element (% wt.)	Fe/Ni electrode	EC	EC-NaClO
F	–	2.54	–
Cl	0.03	10.20	20.20
O	–	44.30	30.70
Na	0.12	5.33	34.80
Fe	61.93	31.10	10.80
Ni	37.65	6.36	1.40
Si	0.11	0.05	1.24
Others	0.16	0.12	0.86

Table S2. Comparison of the degrading performance of PFOA with different processes.

System			Contaminant (mg/L)	Volume (mL)	Removal (%) Time (h)	Ref
Catalyst	Degradation methods	Electrode area (cm²)				
Fe plates	EC	25.0	10.0	600.0	100.0 (6.0 h)	[4]
Fe electrode	EC	8	103.5	500	99.0 (0.8 h)	[5]
BDD electrodes	EC	10.5	0.1	400.0	80.0 (8.0 h)	[6]
Al-Zn electrode	EC	24.0	1.0	–	99.6 (0.4 h)	[7]
zinc plate	EC	72.0	200.0	180.0	100.0 (0.2 h)	[3]
zinc sheet	EC	200.0	200.0	300.0	99.7 (1.7 h)	[2]
Fe plate	EC (H$_2$O$_2$)	83.3	100.0	1000.0	90.0 (1.0 h)	[8]
p-TiSO	EC (sulfate)	16.0	41.4	200.0	97.1 (2.0 h)	[9]
Fe anode	EC (H$_2$O$_2$)	8.0	100.0	400.0	99.0 (1.5 h)	[10]
Fe/Ni foam	**EC (NaClO)**	**6.0**	**100.0**	**100.0**	**95.4 (1.5 h)**	**This study**

Table S3. The parameters of real PFOA-containing wastewater.

Parameter	PFOA (mg/L)	TOC (mg/L)	pH	Cation (mg/L)				Anion (mg/L)			
				Na^+	Mg^{2+}	Ca^{2+}	NH_4^+	F^-	Cl^-	NO_3^-	SO_4^{2-}
Average concentration	58.8	13.9	6.8	17.7	10.3	9.1	30.6	3.5	16.6	61.2	31.3

Table S4. The energy cost for PFOA degradation by the EC and the EC-NaClO process with Fe/Ni foam electrode.

Process	Average voltage (V)	EEC (Wh/L)	ΔM_{exp}(mg)	ΔM_{theo}(mg)	η
EC-30 min	7.9	5.9	71.9	79.3	90.6
EC-90 min	8.4	18.9	217.9	238.0	91.6
EC-NaClO-90 min	7.9/1.6	8.3	62.2	238.0	26.1

Table S5. Acquisition parameters of perfluorocarboxylic acids (PFCAs) during quality testing at different reaction times.

Compound	Formula	Mass (m/z)	Retantion time (min)	EC	Mass fraction (wt%)		
					EC-NaClO (20 min)	EC-NaClO (40 min)	EC-NaClO (60 min)
PFOA	$C_7F_{15}COOH$	412.72	7.63	4.5	2.50	1.29	0.48
PFHpA	$C_6F_{13}COOH$	362.71	5.44	54.86	26.40	12.68	23.21
TP1	$C_6F_{13}H$	319.00	4.94	36.05	18.60	8.30	16.50
PFHxA	$C_5F_{11}COOH$	312.83	4.47	0.95	20.90	12.13	7.68
TP2	$C_5F_{11}H$	269.08	4.53	0.70	14.20	7.20	5.22
PEPeA	C_4F_9COOH	262.88	4.13	2.75	10.09	30.06	6.41
TP3	C_4F_9H	219.10	4.09	0.15	3.60	11.30	2.27
PFBA	C_3F_7COOH	213.07	3.82	0.04	0.01	6.81	12.00
TP4	C_3F_7H	169.10	3.84	−	2.10	7.50	14.49
PFPrA	C_2F_5COOH	163.11	3.67	−	0.60	0.90	5.51
TP5	C_2F_5H	119.01	3.68	−	1.00	1.80	6.10
TFA	CF_3COOH	113.09	2.35	−	−	0.03	0.12
TP6	CF_3H	68.88	2.24	−	−	−	0.01

References

1. C. A. M. Huitle, M. A. Rodrigo, I. Sirés and O. Scialdone, Single and Coupled Electrochemical Processes and Reactors for the Abatement of Organic Water Pollutants: A Critical Review, *Chem. Rev.*, 2015, **115**, 13362-13407.
2. Y. Wang, L. Hui, F. Jin, J. Niu, J. Zhao, B. Ying and L. Ying, Electrocoagulation mechanism of perfluorooctanoate (PFOA) on a zinc anode: Influence of cathodes and anions, *Sci. Total Environ.*, 2016, **557-558**, 542-550.
3. H. Lin, W. Yujuan, N. Junfeng, Y. Zhihan and H. Qingguo, Efficient Sorption and Removal of Perfluoroalkyl Acids (PFAAs) from Aqueous Solution by Metal Hydroxides Generated in Situ by Electrocoagulation, *Environ. Sci. Technol.*, 2015, **49**, 10562-10569.
4. M. K. Kim, T. Kim, T. K. Kim, S. W. Joo and K. D. Zoh, Degradation mechanism of perfluorooctanoic acid (PFOA) during electrocoagulation using Fe electrode, *Sep. Purif. Technol.*, 2020, **247**, 116911.
5. B. Yang, Y. Han, G. Yu, Q. Zhuo, S. Deng, J. Wu and P. Zhang, Efficient removal of perfluoroalkyl acids (PFAAs) from aqueous solution by electrocoagulation using iron electrode, *Chem. Eng. J.*, 2016, **303**, 384-390.
6. P. Mattia, M. S, B. K.W, S. Michat, L. Aneta, R. B and F. K. Sylwia, Electrochemical oxidation of PFOA and PFOS in landfill leachates at low and highly boron-doped diamond electrodes, *J. Hazard. Mater.*, 2021, **403**, 123606.
7. Y. Liu, X. M. Hu, Y. Zhao, J. Wang, M. X. Lu, F. H. Peng and J. Bao, Removal of perfluorooctanoic acid in simulated and natural waters with different electrode materials by electrocoagulation, *Chemosphere*, 2018, **201**, 303-309.
8. S. Singh, S. L. Lo, V. C. Srivastava, Q. Qiao and P. Sharma, Mineralization of perfluorooctanoic acid by combined aerated electrocoagulation and Modified peroxi-coagulation methods, *J. Taiwan. Inst. Chem. E.*, 2021, **118**, 169-178.
9. G. Liu, H. Zhou, J. Teng and S. You, Electrochemical Degradation of Perfluorooctanoic Acid by Macro-porous Titanium Suboxide Anode In the Presence of Sulfate, *Chem. Eng. J.*, 2019, **371**, 7-14.
10. B. Yang, Y. Han, Y. Deng, Y. Li, Q. Zhuo and J. Wu, Highly efficient removal of perfluorooctanoic acid from aqueous solution by H_2O_2-enhanced electrocoagulation-electroflotation technique, *Emerging Contaminants*, 2016, **2**, 49-55.